

Palagonia, Maria Sofia ; Brogioli, Dorianò ; La Mantia, Fabio



Lithium recovery from diluted brine by means of electrochemical ion exchange in a flow-through-electrodes cell

Journal Article as: peer-reviewed accepted version (Postprint)

DOI of this document* (secondary publication): <https://doi.org/10.26092/elib/3656>

Publication date of this document: 14/02/2025

* for better findability or for reliable citation

Recommended Citation (primary publication/Version of Record) incl. DOI:

Maria Sofia Palagonia, Dorianò Brogioli, Fabio La Mantia,
Lithium recovery from diluted brine by means of electrochemical ion exchange in a flow-through-electrodes cell,
Desalination, Volume 475, 2020, 114192, ISSN 0011-9164,
<https://doi.org/10.1016/j.desal.2019.114192>.

Please note that the version of this document may differ from the final published version (Version of Record/primary publication) in terms of copy-editing, pagination, publication date and DOI. Please cite the version that you actually used. Before citing, you are also advised to check the publisher's website for any subsequent corrections or retractions (see also <https://retractionwatch.com/>).

This document is made available under a Creative Commons licence.

The license information is available online: <https://creativecommons.org/licenses/by-nc-nd/4.0/>

Take down policy

If you believe that this document or any material on this site infringes copyright, please contact publizieren@suub.uni-bremen.de with full details and we will remove access to the material.

Lithium recovery from diluted brine by means of electrochemical ion exchange in a flow-through-electrodes cell

Maria Sofia Palagonia, Dorian Brogioli*, and Fabio La Mantia*

Universität Bremen, Energiespeicher- und Energiewandlersysteme,
Bibliothekstraße 1, 28359 Bremen, Germany

Abstract

Lithium is becoming an important raw material due to the expansion of the market of lithium-ion batteries, required for electric vehicles and for stationary energy storage. The current method of lithium extraction is slow, inefficient and it has a strong environmental impact. In the last decade a new technology, called “electrochemical ion pumping”, based on the electrochemical selective capture of lithium cations from the brine, followed by the release of the ions into a so-called “recovery solution”, was proposed. In this work, we developed a flow-through-electrodes reactor, with which it was possible to capture lithium from a diluted solution containing 1 mM LiCl and 1 M NaCl, and concentrate it in a recovery solution. After 9 cycles, it was possible to produce 5 mL of 100 mM LiCl solution with 94% purity starting from more than one liter source solution. We have estimated the energy required by the process, finding that the major contribution is given by the hydraulic energy for pumping the electrolyte through the cell. The evaluation shows that the technology is economically feasible and it can enable a sustainable future production of lithium.

Keywords: lithium, intercalation, electrochemistry, electrochemical ion pumping, extraction of lithium.

1 Introduction

According to forecasts, the market of lithium-ion batteries will expand in the near future due to the envisaged spread of stationary energy storage devices and electric and hybrid vehicles, which are based on lithium-ion battery technology [1]. Currently lithium is mainly extracted from brines available in South America, by means of the so-called lime-soda evaporation process, which uses solar evaporation in order to concentrate the brine. This step is followed by other chemical processes for the final purification of LiCl. This method

is very slow, weather dependent and it produces large amount of chemical wastages [2, 3]. Currently, the lithium global production capacity from brine is 120.5 Ktons/year [2], which, according to the predictions, will not be enough to cover the lithium market demand in the near future [4, 5]. For these reasons, the quest for a faster, cleaner, and more convenient technology has become of great interest.

Various technologies have been proposed in the last two decades [6], the most investigated have been the precipitation of lithium from brines as aluminate [7, 8], the adsorption on lithium selective materials [9, 10, 11, 12], and the liquid-liquid extraction with organic solvents [13, 14, 15]. The main disadvantage of those techniques is the need for chemicals (mostly, acids), either for a preliminary treatment of the brine (for example, changing the pH to increase the selectivity) or to regenerate the active material after the capture.

Electrochemical methods for the extraction of lithium from brine are particularly promising (see Ref. [6] for a comparison with the other technologies). They are based on the “electrochemical ion pumping” concept, consisting in the intercalation of lithium cations from the brine into a lithium selective material. After capturing, the brine in the electrochemical reactor is substituted by a recovery solution, in which lithium cations are released by reversing the direction of the current. After the release of lithium ions, the brine is again flushed into the reactor and the cycle starts from the beginning.

Two intercalation materials have been studied for this application: lithium iron phosphate [16] (LFP) and lithium manganese oxide [17] (LMO). The intercalation mechanism and the performances for lithium extraction have been extensively studied [16, 17, 18, 19]; in particular, it has been shown that in both materials the selectivity for lithium ions is excellent.

In some pioneering works, the lithium intercalating electrode was coupled to a counter-electrode that was splitting water [20, 21], generating oxygen during the lithium capturing and hydrogen during the lithium release. This method has a relatively large energy consumption, mostly due to the thermodynamic energy necessary for water splitting and the difficulty of properly disposing the produced gases. Recently, ion insertion or electrochemical conversion have been proposed as processes occurring at the counter electrode [22], i.e. during lithium capture, the counter-electrode either:

- captures anions (by conversion, with silver/silver chloride electrodes [22, 16], or by insertion in polypyrrole [23, 24, 25]);
- *or* releases a cation (by de-insertion from nickel hexacyanoferrate [26, 17]).

In the latter case, the material must exclude the lithium ions from insertion. In any case, the electro-neutrality of the solution is maintained.

The main advantage of the electrochemical ion pumping technique with respect to the conventional ones is that it does not require the use of chemicals for regenerating the materials, since the driving force of lithium capturing and release is the application of the current.

Until now, research on electrochemical ion pumping for lithium extraction has focused mostly on selection of materials for increasing the lithium selectivity, the concentration of the recovery solution and its purity, and on investigation the reaction efficiency [16, 26, 27, 17, 18, 19]. In our work, we focus on lithium manganese oxide (LMO), as lithium capturing electrode, and $\text{KNi}[\text{Fe}(\text{CN})_6]$, nickel hexacyano ferrate (NiHCF), as a lithium excluding electrode. Both materials have working potentials inside the stability window of water, high cyclability, low price, and fast kinetics. These materials have been already studied for extracting lithium from a brines [16, 26, 28, 17]. NiHCF gives much better performances than Ag/AgCl electrodes, due to the high cost and slow kinetics of the latter [29, 26, 22, 27]. Moreover, it has a larger specific capacity and stability than the polypyrrole used in other studies [23, 24, 25].

Our research focused on the design of a suitable reactor for performing the lithium extraction process. As an alternative to the flow-by scheme [30, 31], here we propose a flow-through electrodes reactor, which improves the transport of ions by advection.

With the aim of increasing the variety of the potential lithium sources, recently we have proposed a reactor design aimed to capture lithium from brines with concentration of LiCl down to 1 mM, using LMO and NiHCF as lithium-capturing and lithium-excluding electrodes respectively [32]. Targeted lithium sources could be geothermal waters or brines produced in saltworks, which have a concentration of lithium down to 7-70 mg/l. In such cases, the electrochemical extraction process is limited by the mass transport in the solution. In order to improve the performances, we thus proposed to increase the mass transport by forcing the flow of the source solution through the porous structure of the electrodes (flow-through electrodes configuration). In particular we investigated the capturing step of the process, focusing on the influence of the flow rate and the brine concentration on the amount of lithium captured by the active material [32]. With optimized working parameters, the reactor was able to extract more than 90% of the lithium present in a 1 mM LiCl source solution [33].

Our previous publications on the flow-through reactor [32, 33] were focused on the capture stage; due to the relatively large dead volume, the release of lithium was not performed in conditions relevant for a real process and thus it was not characterized and discussed. In the present work, we modified the flow-through electrodes reactor, with the aim of studying the release step in conditions similar to the real applications and producing a concentrated solution of LiCl in multiple capture / release cycles. In order to have a high concentration of lithium in the recovery solution and avoid back-mixing, the dead volume of the reactor was minimized by using a compact electrode stack. We are thus now able to fully evaluate the performances of the release stage. We carried out experiments by capturing from a source solution with 1 mM of LiCl and releasing it into 5 mL of recovery solution. We analyzed experimental results in terms of transferred lithium, and both electric and hydraulic energy.

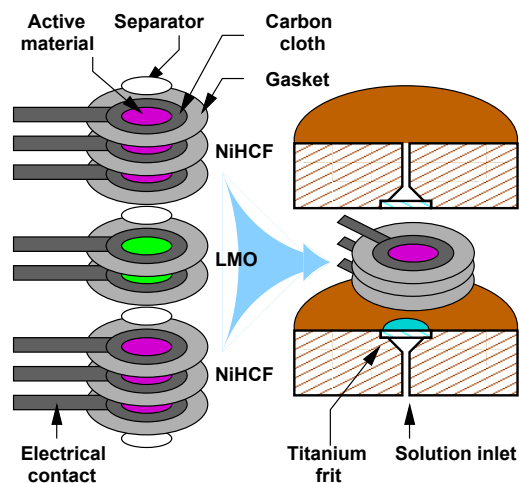


Figure 1: Representation of the electrodes stack (left) and of the cell plates (right).

2 Experimental section

2.1 Electrochemical cell

The flow-through electrodes cell design was aimed at minimizing the dead volume, preventing the back-mixing between the source solution and the recovery solution. The electrode materials used in the cell are LMO and NiHCF. The cell was delimited by two circular plates, pressing the electrode stack (see Fig. 1). The liquid flow takes place through holes in the center of the plates which terminate with a funnel shape, delimited by a titanium frit, directly pressing the electrode stack.

The electrodes are prepared by painting a slurry with the active material on a carbon cloth substrate as current collector (see below for the description); as shown in Fig. 1, they have a circular area of 1.4 cm^2 and a lateral rectangular strip of circa 0.5 cm^2 width, used for electrical connection. Once cut, the edge of each electrode is covered by a ring of silicone rubber, forming a gasket. The circular central part is painted with the active material and remains permeable; it represents the “active area” of the electrode, equal to circa 1.1 cm^2 . When the electrodes are stacked, the active areas are aligned with each another, so that they constitute a porous permeable path through which the liquid flows. The electrode stack is composed by the working electrode (WE) (two short-circuited LMO-painted cloths) placed between two counter electrodes (CE) (each made by three short-circuited NiHCF-painted cloths). Separators made of filter paper, with area 1.1 cm^2 , are placed on each side of the electrodes to prevent short circuits. This “sandwich” configuration was chosen in order to decrease the

Ohmic drop.

2.2 Electrode preparation

LMO powder was supplied by MTI (Richmond, US), and NiHCF powder was synthesized by the co-precipitation method [26]. Briefly, $\text{Ni}(\text{NO}_3)_2 \cdot 6 \text{H}_2\text{O}$ (120 mL, 0.1 M; Sigma-Aldrich) and $\text{K}_3\text{Fe}(\text{CN})_6$ (120 mL, 0.05 M; Sigma-Aldrich) were mixed dropwise in 60 mL water at 70°C while stirring constantly. During the mixing, a brown precipitate formed immediately, which was sonicated for 30 min at 70°C and left to rest overnight. The precipitate was then centrifuged, washed with distilled water, and dried at 60°C.

From the powders, the slurries were prepared as previously reported [32]. They consist of the active material, C65 carbon black (Timcal, specific surface area 62 m²/g), polyvinylidene difluoride (Solef S5130, Solvay), and graphite (Timcal SFG6) with 80:9:9:2 wt.% for the NiHCF electrodes and 80:10:10:0 wt.% for LMO powder electrodes. The powder was dispersed in N-methyl-pyrrolidone and mixed thoroughly for 30 min at 4000 rpm by using an ultra-turrax disperser (Ika).

The electrodes were prepared by hand painting the slurry on the above-described carbon cloth current collectors (thickness 250 μm , provided by Fuel Cell Earth) and subsequently dried at 60°C.

The mass loadings of the electrodes were circa 20 mg/cm² and 14 mg/cm² for LMO and NiHCF, respectively. The ratio of the masses of LMO and NiHCF was 1:2.

The electrodes were electrochemically treated in a 50 mL beaker before putting them into the cell; the LMO was cycled and then completely oxidized in a solution having a composition similar to the brines of Atacama lake (40 mM LiCl, 786 mM NaCl, 100 mM KCl and 70 mM MgCl₂). We used this solution as a “reference solution” to measure the LMO capture capacity before the experiments in the flow-through electrode cell [32]. The NiHCF electrodes were cycled one time in 1 M NaCl solution, ending with full reduction.

2.3 Lithium extraction process

The electrochemical process was performed with a Biologic VSP-300 potentiostat. The used technique is the galvanostatic cycling with potential limitation (GCPL), in which the capturing and release steps consisted in applying of a constant current, while recording the potential difference between the WE and the CE. The constant current is stopped when a given potential is reached.

The solutions are injected in the cell by means of a peristaltic pump (Ecoline VC-MS/CA 4-12, Ismatec). Argon is bubbled in the containers of the solutions in order to remove oxygen.

The lithium extraction process is performed by cyclically repeating the following steps.

Capture The source solution (1 mM LiCl and 100 mM NaCl) is continuously pumped from a stirred beaker to the cell with a flow rate of 15 mL/min.

The solution (150 mL) initially contains 20% more lithium than the maximum amount that could be captured by LMO (based on the capacity evaluated as explained in the previous section). A negative current of 0.5 mA is applied to the cell. The LMO reduction occurs and Li^+ ions are intercalated in its structure. NiHCF is oxidized and Na^+ are de-intercalated from the solid to the liquid.

Cleaning 50 mL of a 120 mM KCl solution are pumped through the cell for rinsing it. Then air is pumped into the cell for remove the solution.

Release Hereafter, 5 mL of recovery solution of initial concentration of 120 mM KCl are pumped inside the cell with a flow rate of 5 mL/min. A positive current of 1 mA is applied and the de-intercalation of Li^+ occurs, together with intercalation of K^+ in NiHCF.

Cleaning The solution is pumped out the cell by an air flow

At the end of the cycle, the source solution is re-injected into the cell and another cycle takes place. It is important to notice that the source solution is changed every cycle, while the same recovery solution is used for consecutive cycles, so that its concentration progressively increases.

2.4 Working parameters

The process parameters (flow rate, current and potential limitation) during the capturing step have been chosen accordingly to previous studies on a similar reactor [32]. In that work, we found that the captured lithium increases linearly with the flow rate, up to a saturation value. Beside, we found that the flow rate at which saturation takes place depends on the applied current, namely it decreases by decreasing the current. The flow rate applied during the capturing step was $\sim 50\%$ higher than the value of saturation flow rate we previously found [33]. The current has been chosen as a trade-off between increasing the amount of captured lithium and decreasing the experiment duration (~ 5 h for these experiments).

One of the aims of the reactor design was to minimize the dead volume. Estimating the volume of the cell plates (0.73 mL) and the liquid volume retained by the electrodes ($0.7 \mu\text{L}/\text{mg}$) and the separators ($10 \mu\text{L}/\text{cm}^2$) measured by weight difference, the total liquid volume contained in the cell is circa 0.82 mL, therefore much smaller than the recovery solution volume (5 mL).

Nine cycles (both capturing and release step) were performed one after the other; in each cycle, the capture was from the same source solution of 1.35 L and the release was to the same recovery solution of 5 mL, so that the concentration progressively increased.

Inductively coupled plasma - optical emission spectrometry (ICP-OES) was used to measure the initial and final concentrations of the solutions. The measurements of the source solution concentrations were performed prior and after each cycle, the measurement of the recovery solution were performed after the I, II, III, V, VII, IX cycles, taking $10 \mu\text{L}$ at the end of each cycle for the analysis.

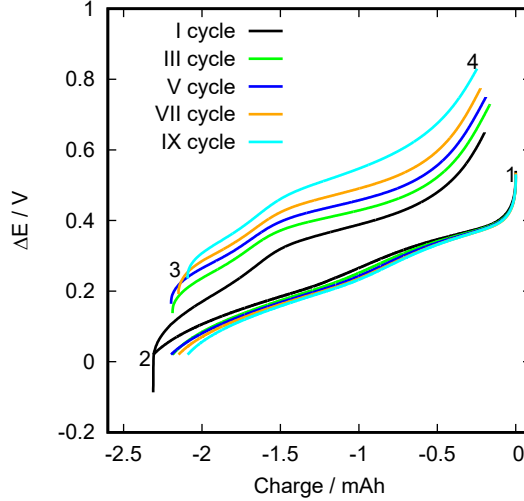


Figure 2: Galvanostatic charge/discharge curves for the I, III, V, and VII cycles. The cycle is composed by two branches: from 1 to 2 (capture) and from 3 to 4 (release). The whole cycle follows the numbers 1, 2, 3, 4, i.e. it runs in clock-wise direction.

3 Results and discussion

3.1 Sequence of cycles

The cell potential difference vs. charge curves for the I, III, V, VII, and IX cycles are reported in Fig. 2. The cycles occur clock-wise, in the direction represented by the numbers 1 (start of capture), 2 (end of capture), 3 (start of release), 4 (end of release): in the bottom curve, from 1 to 2, LMO is reduced and the capturing of lithium from the source solution takes place, in the top curve, from 3 to 4, LMO is oxidized and lithium cations are released into the recovery solution.

The discharging curves (1-2) of all the cycles are almost matching and show a capturing capacity of circa 70% of the reference one. The charging curves (3-4) show higher potentials, which increase with increasing cycle number: this is the expected Nernstian variation of the equilibrium potential due to the increase of the Li^+ concentration in the recovery solution.

By ICP-OES, we measured the concentration of lithium in the various solutions along the sequence of cycles. In the source solution, the initial ($C_{Li,1}$) and final ($C_{Li,2}$) concentrations are 0.91 ± 0.07 and 0.4 ± 0.05 mM, respectively; the uncertainty is attributed to the ICP-OES measurements. This means that approximately 60% of lithium is captured from the source solution during the

Cycle	$C_{Li,3}$	$C_{Li,4}$	$C_{K,3}$	$C_{K,4}$	$C_{Na,4}$	K_{Li}
1	0	15.6	117.5	101.3	0.63	0.13
2	15.6	29.5	101.3	85	1.49	0.25
3	29.5	41.7	85.2	68.1	2.03	0.37
5	-	60.9	-	44.1	6.87	0.54
7	-	80.2	-	8	-	-
9	-	100	-	1	4.84	0.94

Table 1: Initial and final lithium, sodium and potassium concentrations in mM of the recovery solution and purity coefficient of lithium in recovery solution. The subscripts indicate a process stage, corresponding to the numbers reported in the Fig. 2. K_{Li} is the purity (see Eq. 1).

nine cycles. The concentration of Na^+ remains almost constant, due to the high amount of cations in solution with respect to the ones that are de-intercalated from NiHCF.

Initial $C_{i,3}$ and final $C_{i,4}$ concentrations of species i (Li^+ , Na^+ , K^+) in the recovery solution are reported in Table 1.

Li^+ concentration increases upon cycles, reaching a final concentration at the end of the IX cycle of 100 mM. K^+ concentration decreases down to 1 mM. An increase of Na^+ concentration is observed upon cycles, probably due the partial intercalation/adsorption in LMO electrode during the capturing step. C_{Na} of the VII cycle is not reported, as it is out of range.

We also reported the purity coefficients of lithium upon cycles, calculated as the lithium concentration divided by the concentration of all cations in the recovery solution:

$$K_{Li} = \frac{C_{Li}}{\sum_i C_i} \quad (1)$$

The purity coefficient increases upon cycle, reaching a final value of 0.94.

The process involves the intercalation and de-intercalation of two different cations in the two electrode materials: Li^+ in LMO, K^+ in NiHCF. We define the Coulombic efficiencies η , separately for intercalation and de-intercalation, as the ratio between the moles of intercalated (or de-intercalated) cation and the moles of electrons passed through the electrode. We estimated η for the various ions and materials by means of the measured values of the initial and final concentrations of the solutions. For the intercalation processes (intercalation of Li^+ during the capturing step, of K^+ during the lithium release), the Coulombic efficiency is equal to:

$$\eta_{i,c} = \frac{C_{i,start}V - |Q|/F}{C_{i,end}V} \quad (2)$$

where $C_{i,start}$ and $C_{i,end}$ are the starting and final concentrations of the ion i (either Li^+ or K^+) detected by ICP-OES measurements, Q is the net charge passed during the (dis)charge, V is the solution volume. For the de-intercalation process (of Li^+ during the release step and of Na^+ during the lithium capturing

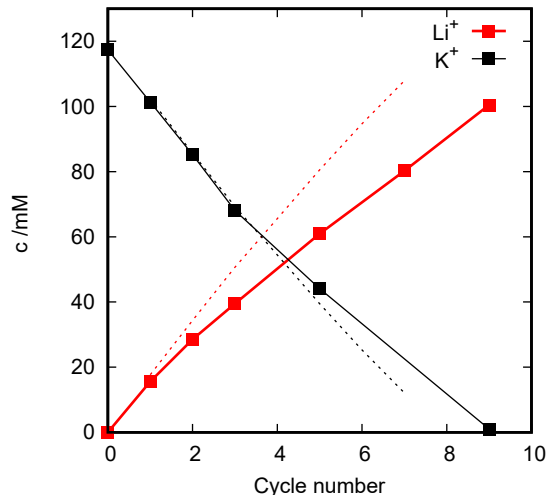


Figure 3: Li^+ and K^+ concentrations in the recovery solution vs. cycles (line with points). The dotted lines are the estimated concentrations by means of the Faraday law with Coulombic efficiency equal to 1.

step), the Coulombic efficiency is equal to:

$$\eta_{i,r} = \frac{C_{i,end}V}{C_{i,start}V + |Q|/F} \quad (3)$$

We estimated an average value of Coulombic efficiency of 0.98 for Na^+ deintercalation and 0.9 for Li^+ intercalation (capturing). The lower value obtained for Li^+ suggests the occurrence of a side reaction on LMO [17].

We reported K^+ and Li^+ concentrations of recovery solution upon cycles in Fig. 3: the lines with points are the experimental values detected with ICP-OES, while the dotted lines are the values evaluated from the circulated charge, assuming a Coulombic efficiency equal to 1. We calculated an overall Coulombic efficiency of the release of $\eta_{overall}=0.75$, evaluated as the ratio between the final experimental Li^+ concentration and the concentration calculated from the circulated charge at the end of the process.

The losses leading to the observed value of $\eta_{overall}$ do not only include the possible side reaction, but are also unwanted back-mixing with the rinsing solution. As already mentioned in the Experimental Section, the rinsing solution is used, between the steps of capturing and releasing. Its composition is the same as the recovery solution at its initial concentration, i.e. 120 mM KCl. Part of this solution remains inside the pores of the electrodes and separators due to capillarity, and is trapped in the dead volume; this solution gets eventually

mixed with the recovery solution when it is injected again in the cell, slightly diluting it and leading to a decrease of the final Li^+ concentration, and an increase of the final K^+ concentration. Considering this effect, given a value of retained volume in the cell V_r , the cation concentrations upon cycles can be calculated as follows:

$$C_{j,\text{Li}} = \frac{C_{j-1,\text{Li}}V + \eta_{\text{Li}^+,r}|Q_j|/F}{V + V_r} \quad (4)$$

$$C_{j,\text{K}} = \frac{C_{j-1,\text{K}}V + C_{r,\text{K}}V_r - \eta_{\text{K}^+,c}|Q_j|/F}{V + V_r} \quad (5)$$

where j is the index of the cycle, Q_j is the net charge passed during the release step, $C_{j,\text{Li}}$ and $C_{j,\text{K}}$ are the final lithium and potassium concentrations and $C_{r,\text{K}}$ is the potassium concentration of the rinsing solution. We reported the concentrations upon cycles evaluated with Eqs. 4 and 5 in Fig. 4, for different values of V_r . We observe a deviation from the linearity for increasing V_r , and a saturation to a maximum value for increasing cycle number.

The higher is V_r , the higher is the dilution effect on Li^+ concentration, and the lower is the cycle number at which the concentration curve reaches the saturation. Indeed after a certain number of cycles, the increase of lithium concentration due to the release by the electrodes is hampered by the decrease due to the dilution. Beside, K^+ concentration increases with V_r , until it starts to increase upon cycles. Hence, a high V_r value has negative effect on both the final concentration and on the purity of the recovery solution; it is therefore fundamental to keep the value of V_r as low as possible.

In order to have a more precise estimation of the dilution effect for our case, choosing a value of V_r (70 μL) and of the Coulombic efficiencies of the electrochemical reactions (0.94 for the capturing of K^+ and 0.8 for the release of Li^+), we estimated the concentrations values versus cycles. They are reported in Fig. 5 (a) (dotted line), and they give a good agreement with the experimental values. The used V_r value corresponds to 1.4% of recovery solution volume. This value is close to the measured volume of the liquid inside the pores of the electrodes and of the separator (90 μL).

By comparing the curves in Fig. 3 and in Fig. 5, we can conclude that in this experimental condition at the IX cycle the saturation of Li^+ concentration is still far. It is thus interesting to extrapolate the curve for more cycles, starting from a more concentrated recovery solution (1 M of KCl); the result is shown in Fig. 5 (b). The curve approaches the saturation at circa 200 cycles, reaching a concentration of 0.8 M of Li^+ .

At the investigated experimental conditions, the total extraction efficiency, evaluated as the final lithium amount in recovery solution (3.45 mg) divided by the total amount in the source solution (9.3 mg) is 37%. This extraction efficiency can be further improved increasing the capture yield. In this experiment, the capture yield is kept to 60%, but it can be optimized up to 90%, by decreasing the applied current, as proved in our previous work [33].

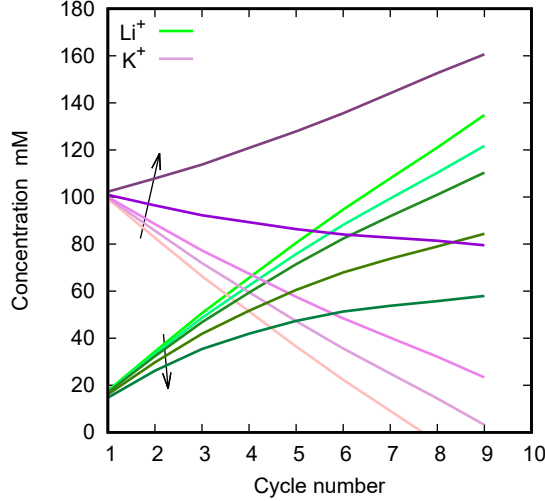


Figure 4: Li^+ and K^+ concentrations evaluated with Eqs. 4 and 5 at various V_r values, namely 0, 0.1, 0.2, 0.5 and 1 mL. The arrows go in the direction of increasing V_r .

3.2 Electrical power estimation

The electrical energy consumption $W_{e,i}$ of the i th cycle is graphically represented by the area enclosed by the cycle in the voltage vs. charge graph (shown in Fig. 2); it is the surface between the charge and the discharge curves:

$$W_{e,i} = \int_{P_{i,1}}^{P_{i,2}} \Delta E(Q) dQ + \int_{P_{i,3}}^{P_{i,4}} \Delta E(Q) dQ \quad (6)$$

where ΔE is the cell voltage, Q is the charge, and the symbols $P_{i,k}$ refer to the four instants $k=1, 2, 3, 4$ of the i th graph, corresponding to the numbers shown on the graph of Fig 2.

The electrical energy consumption $W_{e,i}$ can be divided into two contributions, the reversible and irreversible energies, $W_{rev,i}$ and $W_{irr,i}$, respectively:

$$W_{e,i} = W_{rev,i} + W_{irr,i} \quad (7)$$

The $W_{rev,i}$ term equals the variation of the free energy of the solutions due to the ion pumping. The term $W_{irr,i}$ accounts for the non-reversible processes, such as ohmic drop, charge transfer and diffusion overpotential. Such effects have been recently discussed for a similar electrochemical system by means of mathematical modelling [34].

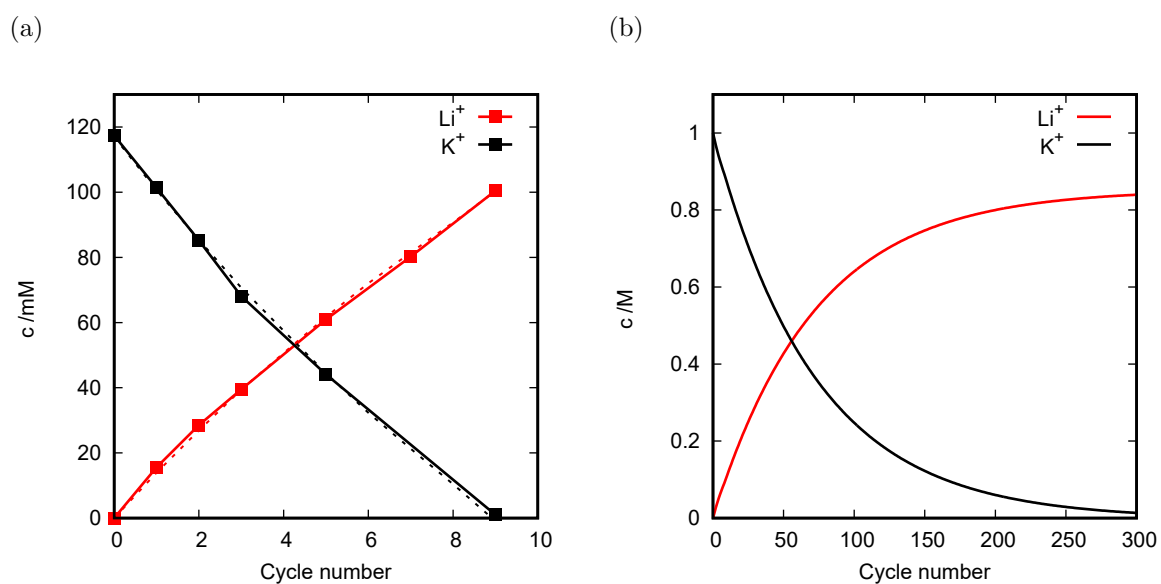


Figure 5: Panel (a): experimental concentrations upon cycles (pointed line) and calculated concentrations (dotted line) with $V_r=70 \mu\text{L}$ and Coulombic efficiencies values of 0.8 and 0.94 for Li^+ and K^+ (de)intercalation respectively. Panel (b): calculated concentrations up to 300 cycles starting from an initial K^+ concentration of 1 M.

While the total $W_{e,i}$ is evaluated from the experimental data, by means of Eq. 6, the two contributions $W_{rev,i}$ and $W_{irr,i}$ are distinguished based on a theoretical evaluation as discussed in the following.

The reversible part, $W_{rev,i}$, equals the free energy variation of the solutions (evaluated under thermodynamic equilibrium) due to the concentration changes, which is induced by the ion pumping operation. It can be calculated by expressing ΔE with the Nernst equation [28]. The Nernst equations for the reactions occurring from point 1 to 2 (capture) and from point 3 to 4 (release) of Fig. 2 are:

$$(1-2) : \Delta E(Q) = \Delta E_1^0 + \Delta E_1'(Q) + \frac{RT}{F} \ln \left[\frac{C_{Li,1} + \frac{Q}{FV_1}}{C_{Na,1} - \frac{Q}{FV_1}} \right] \quad (8)$$

$$(3-4) : \Delta E(Q) = \Delta E_2^0 + \Delta E_2'(Q) + \frac{RT}{F} \ln \left[\frac{C_{Li,3} + \frac{Q-Q_f}{FV_3}}{C_{K,3} - \frac{Q-Q_f}{FV_3}} \right] \quad (9)$$

where Q is a negative number (as in Fig. 2), Q_f is the charge reached at the end of the reduction step (a negative value), and $\Delta E'(Q)$ is the contribution to the potential depending on the state of charge of the electrode. During the capturing step, the change of $C_{Li,1}$ has to be considered, while $C_{Na,1}$ is approximatively constant. Both $C_{Li,3}$ and $C_{K,3}$ change during the release step. ΔE_1^0 and ΔE_2^0 are constant terms depending on the standard potentials of the occurring reactions, namely:

$$\Delta E_1^0 = E_{Li}^{0,LMO} - E_{Na}^{0,NiHCF} \quad (10)$$

$$\Delta E_2^0 = E_{Li}^{0,LMO} - E_K^{0,NiHCF} \quad (11)$$

where $E_{Li}^{0,LMO}$ is the standard potential of intercalation of Li^+ in LMO, $E_{Na}^{0,NiHCF}$ and $E_K^{0,NiHCF}$ are the standard potentials of intercalation in NiHCF of Na^+ and K^+ , respectively.

Substituting Eqs. 8 and 9 in Eq. 6, one obtains:

$$W_{rev,i} = \int_{Q_f}^0 \left\{ \Delta E^0 + \Delta E'(Q) + \frac{RT}{F} \ln \left[\frac{\left(C_{Li,3} + \frac{Q-Q_f}{FV_3} \right) \left(C_{Na,1} - \frac{Q}{FV_1} \right)}{\left(C_{Li,1} + \frac{Q}{FV_1} \right) \left(C_{K,3} - \frac{Q-Q_f}{FV_3} \right)} \right] \right\} dQ \quad (12)$$

where $\Delta E^0 = \Delta E_2^0 - \Delta E_1^0$, $\Delta E'^0 = \Delta E_2'^0 - \Delta E_1'^0$. The charges passing during reduction and oxidation are different due to the limited Coulombic efficiency; we used as Q_f the average value between the two.

While the first term on the integral in Eq. 12 is simply a constant, the integral of the second term is zero. By integrating the second term:

$$\begin{aligned} W_{rev,i} &= -Q_f \left(E_{Na}^{0,NiHCF} - E_K^{0,NiHCF} \right) \\ &\quad - Q_f \frac{RT}{F} \ln \left[\frac{\left(C_{Li,3} - \frac{Q_f}{FV_3} \right) \left(C_{Na,1} - \frac{Q_f}{FV_1} \right)}{\left(C_{Li,1} + \frac{Q_f}{FV_1} \right) \left(C_{K,3} + \frac{Q_f}{FV_3} \right)} \right] \end{aligned} \quad (13)$$

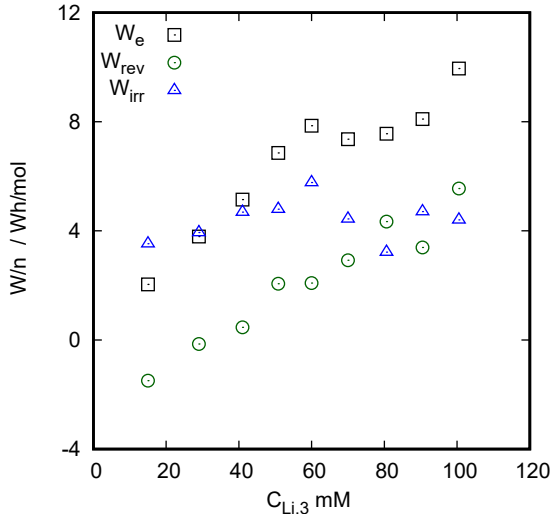


Figure 6: Electrical energy consumption evaluated from the galvanostatic curves, reversible electrical energy consumption evaluated by Eq. 13 and irreversible energy consumption evaluated as difference, per unit of transferred lithium moles.

We have estimated the values of the average intercalation potential of Na^+ and K^+ in NiHCF in our previous paper [29], as $E_{Na}^{0,NiHCF} = 0.381$ and $E_K^{0,NiHCF} = 0.506$ V vs. Ag/AgCl, respectively, in thermodynamic equilibrium condition. This expression is an approximation because it was calculated over the full capacity [29], which is not always the case in our experiments. The approximation is anyway reasonable, as $\Delta E'$ is small compared to the total potential. Since $E_K^{0,NiHCF} > E_{Na}^{0,NiHCF}$, this term decreases the energy consumption $W_{rev,i}$ of the system.

In Fig. 6, $W_{rev,i}$ values for each cycle calculated by Eq 13 are reported. They are calculated using the experimental concentrations of Tab. 1 and the measured charge passed during each cycle. In the same graph the electrical energy consumption, calculated from the integrals of the curves of Fig. 2, are shown. The horizontal axis is $C_{Li,3}$, the concentration in the recovery solution.

The two curves have similar shape, logarithmically increasing with $C_{Li,3}$ [28]. W_{rev} is negative during the first two cycles, until ≈ 30 mM, i.e. the process is thermodynamically spontaneous up to this concentration. This means that, during the first two cycles, the actually consumed energy W_e is lower than the W_{irr} , the difference being extracted from the free energy of the solutions. In general, the increase of (total) electrical energy consumption is almost totally due to the increase of W_{rev} , while W_{irr} remains almost constant.

In Fig. 6, W_e , W_{rev} and W_{irr} (the latter evaluated by Eq. 7) are reported;

in this graph, they are normalized by lithium number moles transferred in each cycle.

The total electrical energy required for the whole sequence of cycles is calculated as:

$$W_T = \sum_j \frac{W_{e,j} N_j}{N_{tot}} \quad (14)$$

where j is the cycle number, N_j are the lithium moles transferred at each cycle, and N_{tot} are the total transferred moles. W_T for this experiment is equal to 6.1 Wh/mol.

The difference $\Delta \bar{E} = E_{Na}^{0, NiHCF} - E_K^{0, NiHCF}$ of Eq. 13 (in this case equal to -130 mV) has a significant effect: it decreases the amount of energy required by the process. Considering the total charge flown into the system ($Q_f \approx 20$ mAh) and the total lithium moles transferred (0.5 mmols), one can estimate that the energy due to this contribution is circa 5.2 Wh/mol. Hence by using KCl instead of NaCl in recovery solution, 85% of energy is spared. This point can be better understood by comparing the mixing free energies of the solutions, before and after the lithium extraction process. We calculate the free energy of the solutions, assuming that they are ideal:

$$G = VC_{Na^+} RT \ln C_{Na^+} + VC_{K^+} RT \ln C_{K^+} + VC_{Li^+} RT \ln C_{Li^+} + VC_{Cl^-} RT \ln C_{Cl^-} \quad (15)$$

where V is the volume of the solution. The lithium extraction process mainly consists in the displacement of Li^+ from the source to the recovery solution and a corresponding displacement of K^+ from the recovery to the source solution. By neglecting the concentration changes of Na^+ and Cl^- , the variation of free energy is:

$$\begin{aligned} \Delta G = & V_{source} C_{K^+,1} RT \ln C_{K^+,1} + V_{source} C_{Li^+,1} RT \ln C_{Li^+,1} + \\ & V_{recovery} C_{K^+,3} RT \ln C_{K^+,3} + V_{recovery} C_{Li^+,3} RT \ln C_{Li^+,3} - \\ & V_{source} C_{K^+,2} RT \ln C_{K^+,2} - V_{source} C_{Li^+,2} RT \ln C_{Li^+,2} - \\ & V_{recovery} C_{K^+,4} RT \ln C_{K^+,4} - V_{recovery} C_{Li^+,4} RT \ln C_{Li^+,4} \quad (16) \end{aligned}$$

This free energy difference appears as an energy saving in our process. It can be split into two terms:

$$\begin{aligned} \Delta G_{Li^+} = & V_{source} C_{Li^+,1} RT \ln C_{Li^+,1} + V_{recovery} C_{Li^+,3} RT \ln C_{Li^+,3} - \\ & V_{source} C_{Li^+,2} RT \ln C_{Li^+,2} - V_{recovery} C_{Li^+,4} RT \ln C_{Li^+,4} \quad (17) \end{aligned}$$

$$\begin{aligned} \Delta G_{K^+} = & V_{source} C_{K^+,1} RT \ln C_{K^+,1} + V_{recovery} C_{K^+,3} RT \ln C_{K^+,3} - \\ & V_{source} C_{K^+,2} RT \ln C_{K^+,2} - V_{recovery} C_{K^+,4} RT \ln C_{K^+,4} \quad (18) \end{aligned}$$

The term ΔG_{Li^+} is negative, because electrical energy must be spent for moving Li^+ from the less concentrated source solution to the more concentrated recovery solution. The passage of K^+ is instead in the direction of a spontaneous process: due to the much larger volume of the source solution, its concentration of K^+ is small during the whole process, thus ΔG_{K^+} is positive. The different volume

explains why $\Delta G_{K^+} > -\Delta G_{Li^+}$, so that the total $\Delta G = \Delta G_{K^+} + \Delta G_{Li^+}$ is positive. On the other hand, ΔG would result negative if Na^+ were used in the recovery solution instead of K^+ , because Na^+ would be pumped from a diluted to a concentrated solution for most of the process.

This discussion shows that the choice of the second cation in recovery solution is an important factor for decreasing the required electrical energy of the process. A related result, which however involved the anions, has been discussed in the LMO/polypyrrole system [25], in which both anions and cations are moved between the solutions; also in that case, the whole process can take place spontaneously when the concentration of the anions in the source solution is much higher than the concentration of lithium.

3.3 Pumping energy

We estimated the hydraulic pumping energy W_p as previously reported [32]:

$$W_p = R_p \Gamma_s^2 T \quad (19)$$

where Γ_s is the volumetric flow, R_p is the hydraulic resistance of the cell, and T is the duration of the process. The value of R_p , measured experimentally, is 130 mbar min/mL (see Ref. [32] for the measurement technique). We obtain $W_p=3200$ and 350 J for the capturing and release step, respectively, corresponding to 1.7 and 0.2 kWh/mol, respectively. The pumping energy W_p required during the capturing step is 9 times larger than the one for the release step, due to the 3 times larger flow rate and the 2 times smaller current. To conclude, the largest energy required by the process, for the extraction of lithium from diluted solution at 1 mM, is the pumping energy during the capture, while the required electric energy (6.1 Wh/mol) is negligible with respect to it.

It is interesting to compare the cost of electricity needed for pumping with the value of the produced lithium. The evaluation of the cost of the electricity is based on a price of 0.097 Euro/kWh, typical of a medium size industrial plant located in Germany [35]. The price of lithium is evaluated from the current price of Li_2CO_3 , around 20 €/kg [1], corresponding to approximately 100 €/kg of lithium content. From these data, we estimate that the pumping energy cost for extracting lithium from 1 mM LiCl brine is around 30% of lithium price, thus the process is economically sustainable. It is worth to remember that the pumping energy depends on the lithium brine concentration, as it roughly decreases with the square of the brine concentration value [32]. Moreover, pumping costs can be further reduced by applying lower current and optimizing the porous structure of the electrode to decrease the hydraulic resistance of the cell [33].

4 Conclusion

In this work we have carried out the lithium extraction from brine by means of an electrochemical ion pumping technique in a flow-through electrodes reactor. We have captured lithium cations from 1.35 L of source solution with 1 mM

LiCl and 100 mM NaCl and released them into 5 mL of recovery solution, reaching a final concentration of lithium of 100 mM LiCl with 94% purity. The release step is realized in the same cell, by changing the hydraulic connections, making the process easily up-scalable, at variance with the previous application of this technology with the same materials [17], where the electrodes had to be manually moved from a cell to another. With respect to the cited previous work, the volume of the release solution has been enlarged by a factor 15. We have optimized the geometry of the cell improving its compactness with respect to our previous works [32, 33], minimizing the dead volume. According to the results, given a good stability of the electrodes upon time, the reactor could reach a final concentration of up to 0.8 M LiCl by performing up to 200 cycles.

We have calculated the electric energy required for the process, distinguishing the reversible (thermodynamic equilibrium) and the irreversible energy consumption. We found that the irreversible energy remains almost constant upon cycles, while the reversible energy consumption increases due to the enrichment of lithium in the recovery solution. Moreover, we observed that the reversible energy consumption of the overall process can be decreased by properly choosing the second cation in the recovery solution. However, the highest contribution to the total energy is given by the pumping energy required by the capturing step. By performing a preliminary economic analysis, based on the cost of energy, we observed that the process is still favorable even at a concentration as low as 1 mM LiCl (7 ppm lithium).

The application of the technology in a flow-through electrodes reactor opens the way to the industrial realization of the lithium recovery from diluted brines and thus to the exploitation of lithium sources that were untapped so far. This technology represents a sound response to the increase in lithium demand envisaged in the next future.

Acknowledgement

The authors gratefully acknowledge the support of the Deutsche Forschung Gesellschaft (DFG) in the framework of the Exzellenzinitiative des Bundes und der Länder (ABPZuK-03/2014).

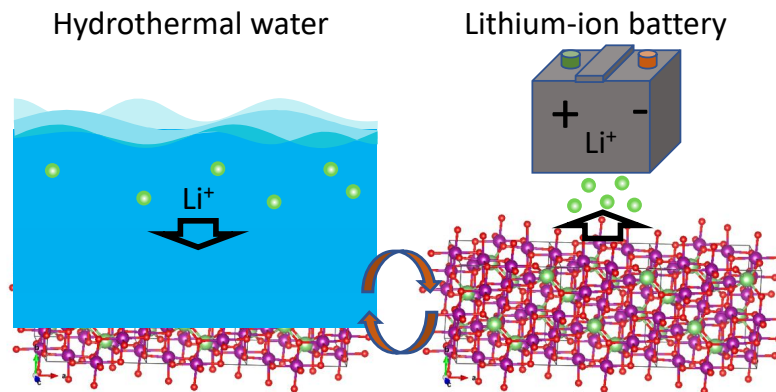
References

- [1] Website of European Lithium, a company that extracts lithium by mining. <http://europeanlithium.com/lithium/lithium-in-europe>, 2018. [online, accessed on 14/10/2019].
- [2] V. Flexer, C. F. Baspinheiro, and C. I. Galli. Lithium recovery from brines: A vital raw material for green energies with a potential environmental impact in its mining and processing. *Science of The Total Environment*, 639:1188–1204, 2018.

- [3] B. Swain. Recovery and recycling of lithium: A review. *Separat. and Purif. Tech.*, 172:388–403, 2017.
- [4] An increasingly precious metal. <http://www.economist.com/business/2016/01/14/an-increasingly-precious-metal>, Gen 2016. [online, accessed on 14/10/2019].
- [5] Cecilia Jamasmie. Lithium demand from battery makers to almost double by 2027. <http://www.mining.com/lithium-demand-battery-makers-almost-double-2027/>, 2018. [online, accessed on 14/10/2019].
- [6] E. J. Calvo. Electrochemical methods for sustainable recovery of lithium from natural brines and battery recycling. *Current Opinion Electrochem.*, 15:102–108, 2019.
- [7] D. Kaplan. Process for the extraction of lithium from dead sea solutions. *Israel Journ. of Chem.*, 1(2):115–120, 1963.
- [8] J.A. Epstein, E.M. Feist, J. Zmora, and Y. Marcus. Extraction of lithium from the dead sea. *J. Appl. Chem. Biotech.*, 6(3-4):269–275, 1981.
- [9] Zandevakili S., Ranjbar M., and Ehteshamzadehc M. Recovery of lithium from Urmia lake by a nanostructure MnO₂ ion sieve. *Hydrometallurgy*, 149:148–152, 2014.
- [10] R. Chitrakar, Y. Makita, K. Ooi, and A. Sonoda. Synthesis of iron-doped manganese oxides with an ion-sieve property: Lithium adsorption from bolivian brine. *Ind. Eng. Chem. Res.*, 53(9):3682–3688, 2014.
- [11] J.-L. Xiao, S.-Y. Sun, J. Wang, P. Li, and J.-G. Yu. Synthesis and adsorption properties of Li₁ · 6 Mn₁ · 6 O₄ spinel. *Ind. Eng. Chem.*, 52:11967–73, 2013.
- [12] M.J. Park, G. M. Nisola, A. B. Beltran, R.Eliseo, C. Torrejos, J. G. Seo, S-P. Lee, H. Kim, and W-J. Chung. Recyclable composite nanofiber adsorbent for Li⁺ recovery from seawater desalination retentate. *Chem. Engin. Journ.*, 254:73–81, 2014.
- [13] Z. Zhou, W. Qin, and W. Fei. Extraction equilibria of lithium with tributyl phosphate in three diluents. *J. Chem. Eng. Data*, 56(9):3518–3522, 2011.
- [14] H. Bukowsky and E. Uhlemann. Selective extraction of lithium chloride from brines. *Sep. Sci. Technol.*, 28:1357–1360, 1993.
- [15] G.G. Gabra and A.E. Torma. Lithium chloride extraction by n-butanol. *Hydrometallurgy*, 3:23–33, 1978.
- [16] R. Trócoli, A. Battistel, and F. La Mantia. Selectivity of a lithium-recovery process based on LiFePO₄. *Chem. Eur. J.*, 20:1810–1813, 2014.

- [17] R. Trócoli, C. Erinmwingbovo, and F. La Mantia. Optimized lithium recovery from brines by using an electrochemical ion-pumping process based on λ - MnO_2 and nickel hexacyanoferrate. *Chem. Electro Chem.*, 4:143–149, 2017.
- [18] F. Marchini, F. J. Williams, and E.J.Calvo. Electrochemical impedance spectroscopy study of the $\text{Li}_x\text{Mn}_2\text{O}_4$ interface with natural brine. *J. Electroanalyt. Chem.*, 819:428–434, 2018.
- [19] F. Marchini, E. J. Calvo, and F. J. Williams. Effect of the electrode potential on the surface composition and crystal structure of LiMn_2O_4 in aqueous solutions. *Electrochimica Acta*, 269:706–713, 2018.
- [20] H. Kanoh, K. Ooi, Y. Miyai, and S. Katoh. Selective electroinsertion of lithium ions into a platinum/lambda-manganese dioxide electrode in the aqueous phase. *Langmuir*, 7:1841–1842, 1991.
- [21] H. Kanoh, K. Ooi, Y. Miyai, and S. Katoh. Electrochemical recovery of lithium ions in the aqueous phase. *Sep. Sci. Technol.*, 28:643–651, 1991.
- [22] M. Pasta, A. Battistel, and F. La Mantia. Batteries for lithium recovery from brines. *Energy Environ. Sci.*, 5:9487, 2012.
- [23] F. Marchini, D. Rubi, M. del Pozo, F. J. Williams, and E. J. Calvo. Surface chemistry and lithium-ion exchange in LiMn_2O_4 for the electrochemical selective extraction of LiCl from natural salt lake brines. *J. Phys. Chem. C*, 120(29):15875–15883, 2016.
- [24] L. L. Missoni, F. Marchini, M. del Pozo, and E. J. Calvo. A LiMn_2O_4 -polypyrrole system for the extraction of LiCl from natural brine. *J. Electrochem. Soc.*, 163(9):A1898–A1902, 2016.
- [25] F. Marchini, F. J. Williams, and E. J. Calvo. Sustainable selective extraction of lithium chloride from natural brine using a $\text{Li}_{1-x}\text{Mn}_2\text{O}_4$ ion pump. *J. Electrochem. Soc.*, 165(14):A3292–A3298, 2018.
- [26] R. Trócoli, A. Battistel, and F. La Mantia. Nickel hexacyanoferrate as suitable alternative to Ag for electrochemical lithium recovery. *ChemSusChem*, 8:2514–9, 2015.
- [27] M. Pasta, C. D. Wessells, Y. Cui, and F. La Mantia. A desalination battery. *Nano Lett.*, 12:839–843, 2012.
- [28] Trócoli R., G. Kasiri Bidhendi, and LaMantia F. Lithium recovery by means of electrochemical ion pumping: a comparison between salt capturing and selective exchange. *J. Phys. Condens. Matter*, 28(11), 2016.
- [29] C. Erinmwingbovo, M. S. Palagonia, D. Brogioli, and F. La Mantia. Intercalation into a prussian blue derivative from solutions containing two species of cations. *ChemPhysChem*, 18:917–925, 2016.

- [30] S. Kim, J. Lee, J.S.Kang, K. Jo, S. Kim, Y. Sung, and J. Yoon. Lithium recovery from brine using a λ -MnO₂/activated carbon hybrid supercapacitor system. *Chemosphere*, 125:50–56, 2015.
- [31] S. Kim, H. Joo, T. Moon, S.H. Kim, and J. Yoon. Rapid and selective lithium recovery from desalination brine using an electrochemical system. *Environmental Science*, 2019.
- [32] M.S. Palagonia, D. Brogioli, and F.La Mantia. Influence of hydrodynamics on the lithium recovery efficiency in an electrochemical ion pumping separation process. *J. Electr. Soc.*, 164(14):E586–E595, 2017.
- [33] M. S. Palagonia, D. Brogioli, and F. La Mantia. Effect of current density and mass loading on the performance of a flow-through electrodes cell for lithium recovery. *J. Electrochem. Soc.* , accepted.
- [34] V. C. E. Romero, M. Tagliacruzchi, V. Flexer, and E. J. Calvo. Sustainable electrochemical extraction of lithium from natural brine for renewable energy storage. *J. Electrochem. Soc.*, 165(10):A2294–A2302, 2018.
- [35] Industrial electricity prices in selected countries in europe 2017, by amount consumed. <https://www.statista.com/statistics/267068/industrial-electricity-prices-in-europe>, 2017.



Capturing lithium Lithium-ion batteries are one of the keys for sustainable energy management, but the supply of lithium itself could become unsustainable. Small amounts of lithium, present in various water sources, can be captured by intercalation in lithium manganese oxide, by means of an electrochemical process, and then released, producing a concentrated and extremely pure solution of a lithium salt, suitable for battery manufacturing.